ELSEVIER

Journal of Power Sources 103 (2002) 273–279

JOURNAL OF POWER SOURCES

www.elsevier.com/locate/jpowsour

Synthesis and electrochemical properties of V_2O_5 intercalated with binary polymers

Nam-Gyu Park[a,*], Kwang Sun Ryu[a], Yong Joon Park[a], Man Gu Kang[a], Dong-Kuk Kim[b], Seong-Gu Kang[c], Kwang Man Kim[a], Soon-Ho Chang[a]

[a]*Telecommunication Basic Research Laboratory, Electronics and Telecommunications Research Institute (ETRI), 161 Kajong-dong, Yusong-gu, Taejon 305-350, South Korea*

[b]*Department of Chemistry, Kyungpook National University, Taegu 702-201, South Korea*

[c]*Department of Chemical Engineering, Hoseo University, Chungnam 336-795, South Korea*

Received 20 May 2001; accepted 13 July 2001

Abstract

We have synthesized a new inorganic/organic hybrid material, which comprises vanadium pentoxide (V_2O_5) and the binary polymers poly(2,5-dimercapto-1,3,4-thiadiazole) (PDMcT) and polyaniline (PANI), and have investigated its electrochemical property. Fourier transform infrared spectra (FT-IR) confirms that both 2,5-dimercapto-1,3,4-thiadiazole (DMcT) and aniline molecules are oxidatively intercalated into the interlayer of V_2O_5 xerogel, and result in a binary polymers/V_2O_5 hybrid material. X-ray diffraction (XRD) shows that intercalation of polymers expands the V_2O_5 interlayer distance by 4.8 Å. V K-edge X-ray absorption near-edge structure spectroscopic analysis shows no significant change in VO_6 octahedral symmetry, but a slight reduction of the V(5+) state. Electrochemical investigations in the 4–2 V range versus Li/Li^+ using non-aqueous electrolyte cells show that as-synthesized binary polymers/V_2O_5 material exhibits an initial discharge capacity of ~190 mAh g^{-1} while an oxygen-treated sample exhibits an initial capacity of about 220 mAh g^{-1} and a better reversibility for lithium insertion/de-insertion.

Keywords: Lithium battery; Intercalation; Hybrid; Vanadium pentoxide; Poly(2,5-dimercapto-1,3,4-thiadiazole); Polyaniline

1. Introduction

Recent research trends in the field of rechargeable lithium batteries are directed towards the development of cells with high specific energy (Wh kg^{-1}) and high energy density (Wh l^{-1}) [1]. To achieve a high amount of energy stored in a given mass or volume, it is usually desirable that the number of available charge carriers per mass or volume unit is as high as possible. The capacity for energy storage in a rechargeable lithium cell is mainly dependent on the cathode materials. The most studied cathode materials for lithium batteries are crystalline cobalt-, manganese- and nickel-based oxides [2]. Although these transition-metal oxides have demonstrated high positive potential and good stability toward long-term cycling for lithium insertion/de-insertion, relatively low discharge capacity and high cost still remain as issues to be addressed.

As part of continuing efforts to improve the capacity of cathode materials, attempts to synthesize transition-metal oxides with an amorphous nature and high surface area, such as the xerogel and aerogel forms, have been made for V_2O_5 [3–7] and MnO_2 [8]. Hybridization of the layered inorganic cathode materials with electrochemically active organic polymers has been regarded as another interesting approach to improving capacity for electrochemical lithium insertion. Inorganic–organic hybrid materials can be produced by intercalating organic molecules into the layered inorganic host materials. Recently, V_2O_5 xerogel hybridized with polyaniline (PANI) or polypyrrole (PPY) has been used as a cathode material in a rechargeable lithium battery [9–15]. Improved capacity was observed for an oxygen-treated PANI/V_2O_5 hybrid material [14]. Except for the conducting polymers, an organic sulfur compound such as 2,5-dimercapto-1,3,4-thiadiazole (DMcT) can be a candidate for the intercalation guest. It was reported that intercalation of dimeric DMcT into V_2O_5 led to a poly(DMcT)/V_2O_5 hybrid material [16]. DMcT is an interesting material because it can be utilized as a charge storage material due to the fact that it undergoes a reversible redox reaction: dimercapatan is polymerized by charging (oxidation) and depolymerized by discharging (reduction). DMcT and PDMcT

* Corresponding author. Tel.: +82-42-860-5680; fax: +82-42-860-6836.
E-mail address: npark@etri.re.kr (N.-G. Park).

0378-7753/02/$ – see front matter
PII: S0378-7753(01)00863-1

are known to be not electronically conductive, but their electrochemical redox process is made highly efficient by conducting PANI [17].

We have been interested in hybridizing electrochemically active organic materials with layer-structured cathode materials. For this purpose, we have chosen V_2O_5 xerogel for the inorganic part and binary DMcT and PANI as organic constituents because both these parts are expected to be active for lithium insertion/de-insertion, as mentioned previously. We have attempted to co-intercalate monomer DMcT and polyanilne into V_2O_5, but found that it is not easy to stabilize DMcT in a monomer form because of the oxidant characteristics of V_2O_5. Instead, polymerized forms of DMcT and aniline have been found to co-intercalate into V_2O_5. In this paper, we report the synthesis, characterization and electrochemical properties of binary polymers/V_2O_5 hybrid materials. We also compare the electrochemical characteristics of the as-prepared hybrid material and a oxygen post-treated one.

2. Experimental

2.1. Preparation of $V_2O_5{\cdot}nH_2O$ xerogel

V_2O_5 xerogels were prepared by dissolving V_2O_5 (3 g) in 10% hydrogen peroxide (300 ml) at ambient temperature [18]. An exothermic reaction took place during a partial decomposition of H_2O_2 leading to the release of oxygen gas. A clear orange solution was formed after about 10 min, and turned into a dark red gel after few hours. The red gel, after ageing for 3 days, was dried at 100°C and gave a compound of $V_2O_5{\cdot}nH_2O$ ($n \approx 1.8$), where the water content was deduced from the observed interlayer distance ($d \approx 11.8$ Å) from X-ray diffraction (XRD) analysis, and was consistent with the findings of other studies [19,20].

2.2. Synthesis of (PDMcT + PANI)/V_2O_5 hybrid materials

A total of 0.17 g (1.17 mmol) of DMcT was dissolved in 240 ml of methanol. To this was added 0.5 g (2.34 mmol) of dried V_2O_5 xerogel dissolved in 30 ml of water. The mixture was stirred at room temperature for 1 h, and then 0.22 g (2.34 mmol) of aniline was added. The reaction mixture was stirred at room temperature for 24 h in air. The product was isolated by filtration and washed with methanol until the yellow color of the filtrate disappeared. The resulting green powder was dried at 50°C under vacuum.

2.3. Synthesis of PDMcT/V_2O_5 and PANI/V_2O_5 hybrid materials

As reference samples, PDMcT/V_2O_5 and PANI/V_2O_5 hybrid materials were prepared. For intercalation of PDMcT into V_2O_5, monomer DMcT was used as a starting chemical instead of the dimer form as described in literature [16]. A total of 0.5 g (2.34 mmol) of dried V_2O_5 xerogel was mixed with 30 ml of H_2O solution, and then added to 0.17 g (1.17 mmol) DMcT dissolved in 240 ml of methanol. A green solution appeared immediately. The reaction mixture was kept at room temperature in air with constant stirring for 24 h. The resulting brown powder was filtered and washed with methanol, and then dried at 50°C under vacuum.

Intercalation of polyaniline into V_2O_5 was performed by reacting V_2O_5 xerogel with aniline in a methanol:water (80:20 wt.%) solution. A total of 0.5 g (2.34 mmol) of dried V_2O_5 xerogel was mixed with 30 ml of water, which was added to a 0.22 g (2.34 mmol) of aniline solution dissolved in 240 ml of methanol. The reaction mixture was stirred at room temperature for 24 h. The resulting black powder was washed with methanol followed by drying at 50°C under vacuum.

2.4. Oxygen post-treatment

Oxygen post-treatment was carried out by heating the as-prepared samples at 100°C for 3 h under a constant flow of oxygen in a tubular furnace.

2.5. Characterization

Powder XRD analysis was performed by means of a Rigaku X-ray diffractometer in the 2θ range from 3 to 60° with Cu Kα radiation ($\lambda = 1.5406$ Å). Fourier transform infrared spectra (FT-IR) were recorded as KBr pellet with a MAGNA-IR 560 spectrometer (Nicolet). The V K-edge X-ray absorption spectra were recorded at beamline EXAFS3C1 at the Pohang Accelerator Laboratory (PAL), operated at 2.5 GeV with ca. 100 ∼ 150 mA of stored current. A Si(3 1 1) double crystal monochromator was employed to collect high resolution X-ray absorption near edge structure (XANES) spectra. The absorption energy was calibrated by simultaneously measuring the V K-edge XANES spectrum for a vanadium metal foil. All XANES spectra were recorded in the transmission mode. Analyses of the experimental spectra were performed by the following standard procedure The inherent background in the data was removed by fitting a polynomial to the pre-edge region and extrapolation through the entire spectrum, from which it was subtracted. The absorption, $\mu(E)$, was normalized to an edge jump of unity.

2.6. Electrochemical characterization

Electrochemical studies were carried out using A Macpile-II galvanostat system under a constant current density of 0.5 mA cm^{-2} in the 4–2 range. A Swagelok-type cell [21] was assembled in the dry room. The mixture of synthesized organic/V_2O_5 material, Super P black (MMM Carbon Co.) and polytetrafluoroethylene (70:20:10 wt.%) was used as the cathode, lithium foil as the anode, and 0.95 M solution of $LiPF_6$ in ethylene carbonate/dimethyl carbonate (50:50 vol.%) as electrolyte.

3. Results and discussion

3.1. Charaterization of binary polymers/V_2O_5 hybrid materials

The FT-IR spectra of the V_2O_5 xerogels before and after intercalation are shown in Fig. 1. The FT-IR spectrum of the compound obtained by reacting V_2O_5 xerogel with DMcT (Fig. 1b) shows a strong doublet at around 1045 and 1380 cm^{-1} that is characteristic of polymerized DMcT [16]. In case of intercalating aniline into V_2O_5, bands appear in the 1000–1800 cm^{-1} range and correspond to the typical polyaniline IR pattern (see Fig. 1d), which can be assigned to an emeralidine form [22]. Co-intercalation of DMcT and aniline results in the formation of both PDMcT and PANI, as clearly seen in Fig. 1c. This indicates the co-existence of polymerized dimercaptan and aniline in the host V_2O_5 matrix. The three strong bands below 1000 cm^{-1} are characteristic of vanadium–oxygen stretching [23]. That is, the bands at around 510 and 760 cm^{-1} are due to symmetric and asymmetric V–O–V stretching, respectively, and that at about 1010 cm^{-1} to vanadyl V=O stretching. The positions of the V–O–V vibration bands in the organic/V_2O_5 hybrid compounds are similar to those in the V_2O_5 xerogel, which implies that the in-plane V–O–V bonding character is not significantly altered by intercalation. On the other hand, the vanadyl V=O vibration band of 1015 cm^{-1} in the V_2O_5 xerogel, which is probably sensitive to the out-of-plane chemical environment, shifts down to 1000 and 1005 cm^{-1} for PANI/V_2O_5 and (PDMcT + PANI)/V_2O_5, respectively. By contrast, no chemical shift is observed for PDMcT/V_2O_5. The chemical shift in vanadyl stretching could be related to reduction of the vanadium ions and/or chemical interaction between the intercalants and the host framework. The monomer organic intercalants are all oxidatively polymerized by the intercalation reaction, which means that V_2O_5 is likely to be reduced. If the vanadyl stretching is affected by reduction of vanadium ions, its position should be altered for all of the synthesized organic/V_2O_5 hybrid materials. The PDMcT/V_2O_5 case is not subject to this hypothesis because there is no chemical shift in the vanadyl stretching. Therefore, the chemical shift in vanadyl vibration seems to be sensitive to the interaction process.

The red-shifts for polyaniline-contained intercalates can be, thus, explained by a bonding interaction between the polyaniline and the inorganic lattice, via $N{-}H\cdots O{=}V$ [10]. No chemical shift in $\nu_{C=O}$ observed for the PDMcT-intercalated sample is attributed to the absence of hydrogen bonding associated with almost no protons in PDMcT.

Powder XRD patterns of the V_2O_5 xerogels before and after intercalation are given in Fig. 2. The XRD analysis confirms the intercalation of organic polymers into the interlayer of V_2O_5 xerogel from the lower angle-shifted (0 0 1) reflections upon intercalation. Interlayer expansion from 11.79 to 13.83 Å is observed for all the organic polymer-intercalated samples. This interlayer expansion of about 2 Å is in good agreement with previous reports on PANI/V_2O_5 [14,22] and PDMcT/V_2O_5 [16]. The expansion is a consequence of removing one layer of H_2O (approximately 2.8 Å) and inserting one monolayer of PDMcT and/or PANI. The net interlayer expansion can, thus, be calculated to be 4.8 Å, which suggests that parallel polymer chains lie between the V_2O_5 slabs [22]. In the case of the (PDMcT + PANI)/V_2O_5 system, the exact structure of the intercalated binary PDMcT and PANI polymers cannot

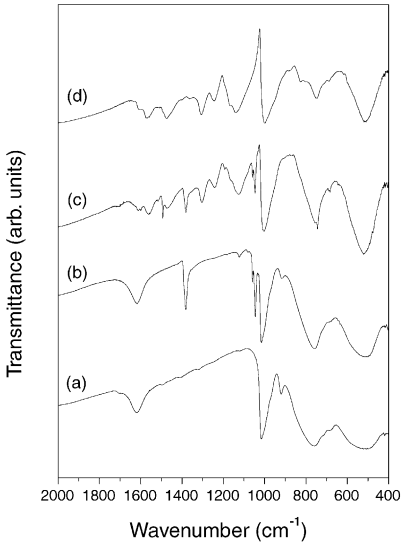

Fig. 1. FT-IR spectra of as-prepared: (a) V_2O_5 xerogel; (b) PDMcT/V_2O_5; (c) (PDMcT + PANI)/V_2O_5; (d) PANI/V_2O_5.

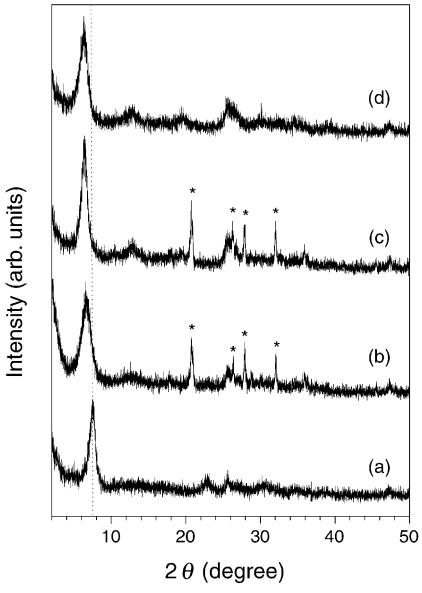

Fig. 2. Powder X-ray diffraction patterns of as-prepared: (a) V_2O_5 xerogel; (b) PDMcT/V_2O_5; (c) (PDMcT + PANI)/V_2O_5; (d) PANI/V_2O_5. Peaks marked with asterisks in spectra (b) and (c) are associated with PDMcT.

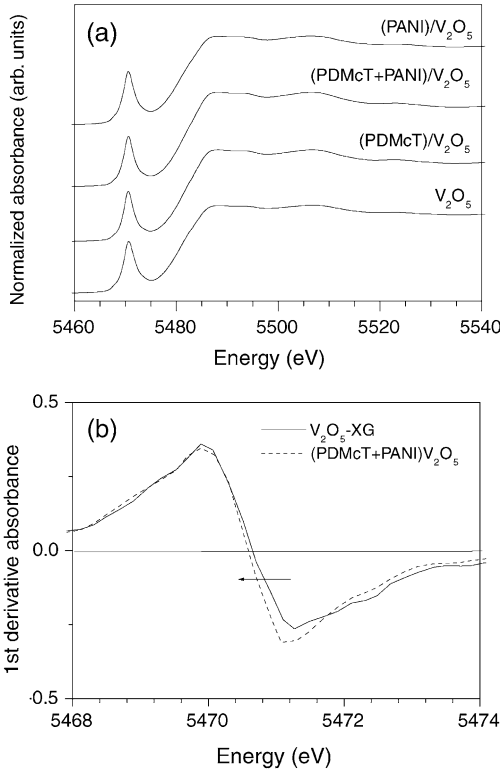

Fig. 3. (a) Normalized vanadium K-edge XANES spectra of V_2O_5 xerogel and its intercalates; (b) first-derivative vanadium K-edge XANES spectra of V_2O_5 xerogel and (PDMcT + PANI)/V_2O_5, showing a red-shift in pre-edge upon intercalation of binary polymers.

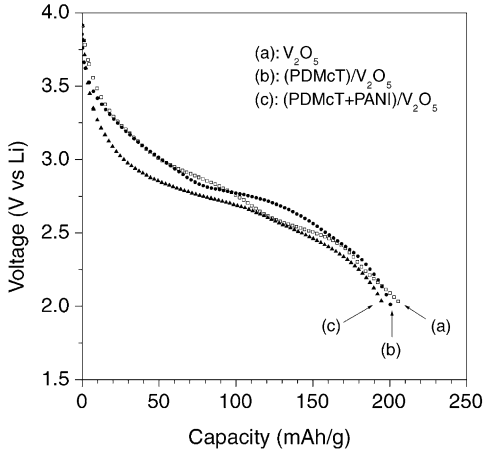

Fig. 4. First discharge curves of as-prepared: (a) V_2O_5; (b) PDMcT/V_2O_5; (c) (PDMcT + PANI)/V_2O_5. Data were collected under constant current density of 0.5 mA cm^{-2} in 4–2 V range.

be resolved from the powder XRD, but they may he randomly distributed in the V_2O_5 interlayer.

To investigate the modification of the electronic and local structures of the V_2O_5 xerogels before and after intercalation, XANES spectroscopic studies have been performed. The XANES spectra at the V K-edge for the V_2O_5 xerogel and its organic hybrid compounds are presented in Fig. 3. The similarity of the XANES spectral features before and after intercalation (Fig. 3a) indicates little change in chemical bonding nature around vanadium ions. The strong pre-edge peak due to the 1s → 3d transition at around 5471 eV is typical of vanadium oxides, where its intensity and energy position are associated with the deviation from octahedral symmetry as well as an effective oxidation state of vanadium. The pre-edge peak intensities of the polymer-intercalated samples are almost the same as that of V_2O_5. This implies little modification of the vanadium local symmetry upon intercalation. In the first derivative XANES spectra (Fig. 3b), however, the pre-edge position of (PDMcT + PANI)/V_2O_5 shifts very slightly to a lower energy by about 0.2 eV compared with that for V_2O_5, which indicates partial reduction of vanadium. It was reported that the vanadium XANES pre-edge position decreases linearly with decreasing oxidation state according to the relation $\Delta(E - E_0)/\Delta(x - 5) = 1.1$, where E and E_0 represent the pre-edge energy at the oxidation state of x and the pre-edge energy of the V(5+) state, respectively [24]. From this basis, one can deduce the vanadium oxidation state of the binary polymers-intercalated V_2O_5 but this may not be quantitatively determined because 0.2 eV is within the experimental error.

3.2. Electrochemical characteristics

The first discharge curve for the (PDMcT + PANI)/V_2O_5 together with those for the as-prepared V_2O_5 xerogel and PDMcT/V_2O_5 are given in the Fig. 4. The discharge capacities of both PDMcT- and (PDMcT + PANI)-intercalated V_2O_5 samples are slightly lower than that of the unintercalated V_2O_5 xerogel, i.e. 205 mAh g^{-1} for the as-prepared V_2O_5 xerogel versus 200 and 187 mAh g^{-1} for PDMcT/V_2O_5 and (PDMcT + PANI)/V_2O_5, respectively. This tendency for such a small decrease in discharge capacity has been observed previously for as-prepared organic/V_2O_5 hybrid materials [9,10,12,13]. This might be due to a decreased average vanadium oxidation state as a result of the intercalation of organic polymers and/or poor electroactivity of intercalated polymers toward lithium insertion. As can be seen in Fig. 5, however, oxygen post-treatment increases the discharge capacity by 10 and 17% for PDMcT/V_2O_5 and (PDMcT + PANI)/V_2O_5, respectively. No effect of oxygen post-treatment has been observed in the case of pristine V_2O_5 xerogel. For the polymer-intercalated samples, it is evident that oxygen treatment plays a role in activating PDMcT and/or PANI as an electrochemical active species for lithium insertion. Similarly, the effect of oxygen treatment has been observed for PANI/V_2O_5 [9,10,14] and PPY/V_2O_5 [12,13] systems. The improved discharge capacity by oxygen treatment is probably due to the fact that the reduced V_2O_5 is partially re-oxidized, and polymer chains inside the V_2O_5 gallery couple oxidatively form longer chains, as reported previously [22]. We also observe from the first derivative V K-edge XANES spectra (not shown)

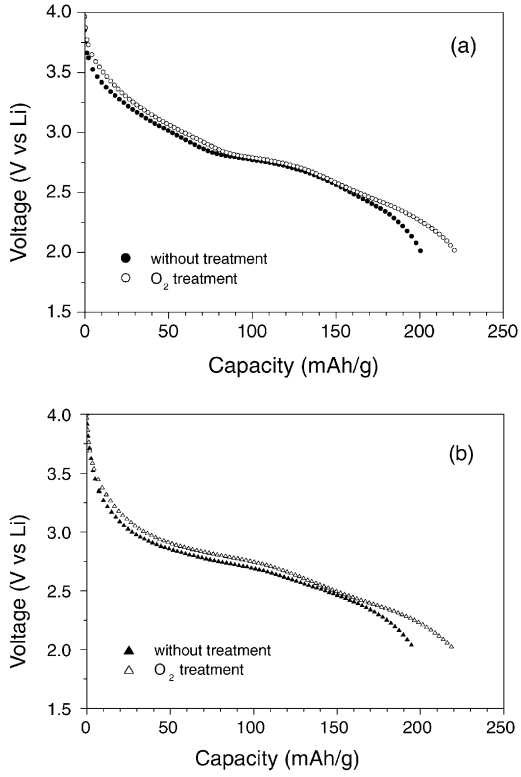

Fig. 5. Effect of oxygen post-treatment on first discharge capacity for (a) PDMcT/V_2O_5; and (b) (PDMcT + PANI)/V_2O_5. Data were collected under constant current density of 0.5 mA cm^{-2} in 4–2 V range.

that the oxygen post-treatment leads to re-oxidation of vanadium ions in the organic/V_2O_5 hybrid compounds.

The contribution of the intercalated organic polymers and V_2O_5 to the total discharge capacity is examined by analysis of the incremental capacity dQ/dV curves that are obtained by numerical differentiation which gives rise to curves similar to cyclic voltammograms [9]. The dQ/dV curves for the first and second discharges of V_2O_5 are shown in Fig. 6. The potential sites of 2.54 and 2.9 V are in good agreement with those reported previously [12–14]. The same peak potentials appear in the second discharge process which indicates electrochemically reversible lithium insertion/de-insertion into V_2O_5. Fig. 7 compares the dQ/dV curves of the as-prepared PDMcT/V_2O_5 and (PDMcT + PANI)/V_2O_5 samples. The curve profiles are quite different from that of V_2O_5. For the case of PDMcT/V_2O_5, the dQ/dV curve calculated from the first discharge data (see upper curve in Fig. 7a) is similar to the previous cyclic voltammograms observed versus Ag/AgCl [16]. A strong dQ/dV peak at 2.78 V that is related to a reduction of PDMcT [16] disappears during the second discharge process (see lower curve in Fig. 7a), which implies that PDMcT in the as-prepared sample is no longer electrochemically reversible for lithium insertion/de-insertion. For the first discharge dQ/dV curve of (PDMcT + PANI)/V_2O_5 in Fig. 7b, the intense peak at around 2.7 V with a shoulder is associated with reduction of PDMcT because its potential is similar to the

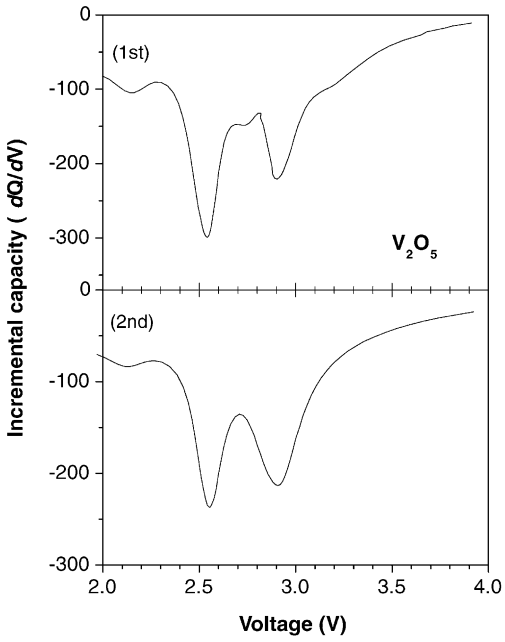

Fig. 6. Incremental capacity (dQ/dV) curves calculated from corresponding first (upper) and second (lower) discharge curves of V_2O_5 xerogel.

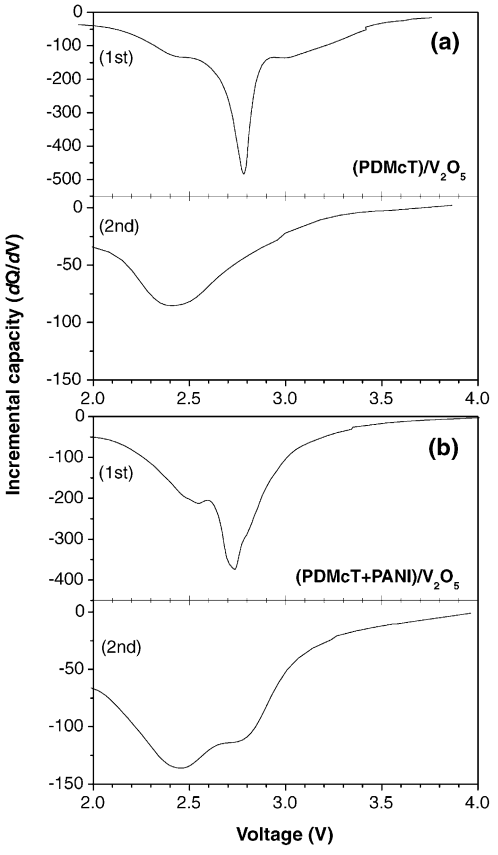

Fig. 7. Incremental capacity (dQ/dV) curves calculated from corresponding first (upper) and second (lower) discharge curves of (a) as-prepared PDMcT/V_2O_5; (b) as-prepared (PDMcT + PANI)/V_2O_5.

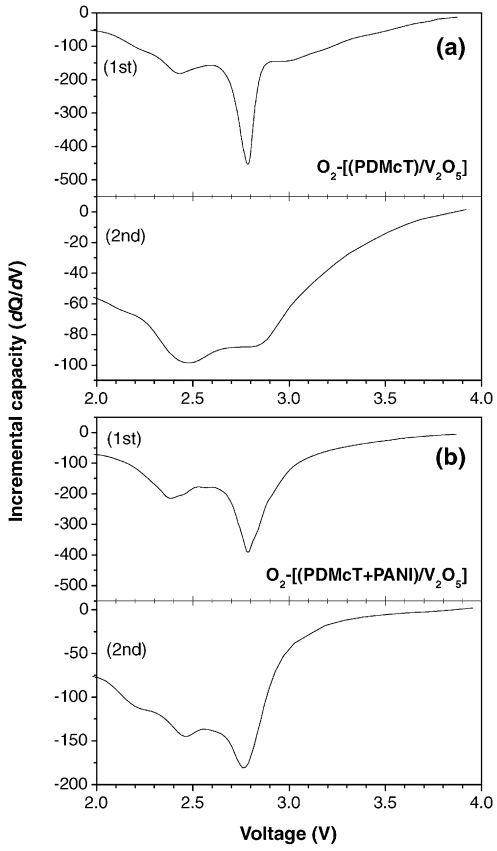

Fig. 8. Incremental capacity (dQ/dV) curves calculated from corresponding first (upper) and second (lower) discharge curves of (a) oxygen post-treated PDMcT/V_2O_5; (b) oxygen post-treated (PDMcT + PANI)/V_2O_5.

potential observed in PDMcT/V_2O_5. The peak at around 2.5 V might be related to the PANI, activity as mentioned previously [14]. The intense peak is weakened with broadened during the second discharge process, which indicates that the intercalated PDMcT is in part still electrochemically active for lithium insertion.

The effect of oxygen post-treatment on the incremental capacity is demonstrated in Fig. 8. The potential sites and curve features of the first discharge dQ/dV curve for the oxygen-treated PDMcT/V_2O_5 (Fig. 8a) are similar to those for the sample without oxygen treatment. Contrary to the as-prepared sample, however, the peak at around 2.8 V does not disappear but broadens with decreased intensity during the second discharge process. This suggests that an electrochemical reversibility of the intercalated PDMcT is promoted by oxygen treatment. The reversibility of PDMcT for lithium insertion/de-insertion is significantly improved by oxygen treatment when it is coupled with PANI, as clearly seen in the second dQ/dV curve of Fig. 8b. Although the reduction and oxidation mechanism of the intercalated binary polymers is not apparent here, the presence of PANI and/or oxygen post-treatment appears to play an important role in the activity of PDMcT towards electrochemical lithium insertion/de-insertion.

4. Conclusions

Binary polymers of PDMcT and PANI are co-intercalated into V_2O_5 xerogel. The intercalation is confirmed by X-ray diffraction and FT-IR. A XANES spectroscopic study shows partial reduction of vanadium ions by co-intercalation. The as-prepared (PDMcT + PANI)/V_2O_5 exhibits a slightly lower discharge capacity than the pristine V_2O_5. Oxygen post-treatment of the hybrid material leads, however, to an improvement in discharge capacity. The studies on an incremental capacity as a function of voltage show that the intercalated PDMcT acts as an electrochemical active species for lithium insertion/de-insertion when it is coupled with PANI and treated with oxygen. We are presently studying the redox mechanism of the intercalated binary polymers, together with attempting to improve further the electrochemical activity of the PDMcT/PANI couple in an inorganic matrix for lithium insertion/de-insertion.

Acknowledgements

This work was supported by the Ministry of Information and Communication of Korea (N.G.P., K.M.K., K.S.R., Y.J.P., and S.H.C.).

References

[1] B.B. Owens, W.H. Smyrl, J.J. Xu, J. Power Sources 81-82 (1999) 150.
[2] M. Winter, J.O. Besenhard, M.E. Spahr, P. Novak, Adv. Mater. 10 (1998) 725.
[3] D.B. Le, S. Passerini, A.L. Tipton, B.B. Owens, W.H. Smyrl, J. Electrochem. Soc. 142 (1995) L102.
[4] D.B. Le, S. Passerini, J. Guo, J. Ressler, B.B. Owens, W.H. Smyrl, J. Electrochem. Soc. 143 (1996) 2099.
[5] F. Coustier, S. Passerini, W.H. Smyrl, J. Electrochem. Soc. 145 (1998) L73.
[6] S. Passerini, J.J. Ressler, D.B. Le, B.B. Owens, W.H. Smyrl, Electrochim. Acta 44 (1999) 2209.
[7] B.B. Owens, S. Passerini, W.H. Smyrl, Electrochim. Acta 45 (1999) 215.
[8] J.J. Xu, A.J. Kinser, B.B. Owens, W.H. Smyrl, Electrochem. Solid State Lett. 1 (1998) 1.
[9] F. Leroux, B.E. Koene, L.F. Nazar, J. Electrochem. Soc. 143 (1996) L181.
[10] F. Leroux, G. Goward, W.P. Power, L.F. Nazar, J. Electrochem. Soc. 144 (1997) 3886.
[11] J. Harreld, H.P. Wong, B.C. Dave, B. Dunn, L.F. Nazar, J. Non-crystalline Solids 225 (1998) 319.
[12] H.P. Wong, B.C. Dave, F. Leroux, J. Harreld, B. Dunn, L.F. Nazar, J. Mater. Chem. 8 (1998) 1019.
[13] G. Goward, F. Leroux, L.F. Nazar, Electrochim. Acta 43 (1998) 1307.
[14] M. Lira-Cantú, P. Gomez-Romero, J. Electrochem. Soc. 146 (1999) 2029.
[15] J.H. Harreld, B. Dunn, L.F. Nazar, Int. J. Inorg. Mater 1 (1999) 135.
[16] E. Shouji, D.A. Buttry, Langmuir 15 (1999) 669.
[17] N. Oyama, T. Tatsuma, T. Sato, T. Sotomura, Nature 373 (1995) 598.
[18] B. Alonso, J. Livage, J. Solid State Chem. 148 (1999) 16.

[19] P. Aldebert, N. Baffier, N. Gharbi, J. Livage, Mater. Res. Bull. 16 (1981) 669.
[20] J.J. Legendre, P. Aldebert, N. Baffler, J. Livage, J. Colloid Interface Sci. 94 (1983) 84.
[21] D. Guyomard, J.M. Tarascon, J. Electrochem. Soc. 139 (1992) 937.
[22] C.-G. Wu, D.C. DeGroot, H.O. Marcy, J.L. Schindler, C.R. Kannewurf, Y.-J. Liu, W. Hirpo, M.G. Kanatzidis, Chem. Mater. 8 (1996) 1992.
[23] M.G. Kanatzidis, C.-G. Wu, J. Am. Chem. Soc. 114 (1989) 4141.
[24] M. Giorgetti, S. Passerini, W.H. Smyrl, S. Mukerjee, X.Q. Yang, J. McBreen, J. Electrochem. Soc. 146 (1999) 2387.